

Multiple stages classification of Alzheimers disease based on structural brain networks using Generalized Low Rank Approximations (GLRAM)

Zhan L, Nie Z, Ye J, Wang Y, Jin Y, Jahanshad N, Prasad G, de Zubicaray GI, McMahon KL, Martin NG, Wright MJ, Thompson PM

Abstract To classify each stage for a progressing disease such as Alzheimers disease is a key issue for the disease prevention and treatment. In this study, we derived structural brain networks from diffusion-weighted MRI using whole-brain tractography since there is growing interest in relating connectivity measures to clinical, cognitive, and genetic data. Relatively little work has used machine learning to make inferences about variations in brain networks in the progression of the Alzheimers disease. Here we developed a framework to utilize generalized low rank approximations of matrices (GLRAM) and modified linear discrimination analysis for unsupervised feature learning and classification of connectivity matrices. We apply the methods to brain networks derived from DWI scans of 41 people with Alzheimers disease, 73 people with EMCI, 38 people with LMCI, 47 elderly healthy controls and 221 young healthy controls. Our results show that this new framework can significantly improve classification accuracy when combining multiple datasets; this suggests the value of using data beyond the classification task at hand to model variations in brain connectivity.

Zhan, Jin, Jahanshad, Prasad and Thompson
Imaging Genetics Center, Department of Neurology, Keck School of Medicine, University of Southern California, Los Angeles, CA 90089, USA, e-mail: zhan.liang@gmail.com

Nie, Ye and Wang
School of Computing, Informatics, and Decision Systems Engineering, Arizona State University, Tempe, AZ, USA

de Zubicaray and McMahon
fMRI Laboratory, University of Queensland, Brisbane, Australia

Martin and Wright
Berghofer Queensland Institute of Medical Research, Australia

The final publication will be available at <http://link.springer.com/book/10.1007/978-3-319-11182-7>. Computational Diffusion MRI. MICCAI Workshop, Boston, USA, September 18, 2014.. L. O'Donnell, G.Nedjati-Gilani, Y. Rathi, M. Reisert, and T. Schneider. (Eds.), Springer-Verlag 2015.

1 Introduction

Alzheimer’s disease is by far the leading form of dementia. There is no cure for the disease, which worsens as it progresses, and eventually leads to death. According to the studies of Alzheimers Disease Neuroimaging Initiative (ADNI) and other large-scale multicenter studies, this disease has been described into four stages: health control (HC); early mild cognitive impairment (EMCI), late mild cognitive impairment (LMCI) and Alzheimers disease (AD)[1, 2, 3]. HC means there is no sign/clue that subject have any cognition impairment, while EMCI and LMCI are the middle stages in time for disease detection. AD is the last stage when there is clearly clue that disease has been onset. Defining atrisk stages of this disease is crucial for predementia detection, which in turn is the requirement for future predementia treatment. In literature, the Alzheimers disease multiple stages classification is mainly based on subjective questionnaire[1, 4]. Here we adopted machine learning method to explore multiple stages automatic classification using diffusion-weighted MRI (DW-MRI).

DW-MRI is a non-invasive brain imaging technique, sensitive to aspects of the brains white matter microstructure that are not typically detectable with standard anatomical MRI.[5] With DWI, anisotropic water diffusion can be tracked along the direction of axons using tractography methods. When tractography is applied to the entire brain, one can reconstruct major fiber bundles and describe connectivity patterns in the brains anatomical network [6]. Brain networks and topological measures derived from them have been shown to be highly associated with aspects of brain function and clinical measures of disease burden [7]. Some studies have begun to apply machine learning techniques to identify network features that differentiate people with various neurological and psychiatric disorders from matched HC [8]. However, most studies focus only on identifying abnormal connectivity patterns in a single disease, compared to controls, and not intermediate stages of the disease, using only using one dataset to do so. While this may improve our understanding of the outcome of the disease, when applying the same analysis to a new disease or a new dataset, the model must be re-trained and re-evaluated. Often, disease effects (or effects of other predictors on brain networks) are subtle and may not be detected in one dataset alone, or may show conflicting results across datasets. In this light, consortia such as Enhancing Neuro Imaging Genetics through Meta-Analysis (Enigma) have been formed to jointly analyze over 20,000 brain scans from patients and controls scanned at over 100 sites worldwide to meta-analyze effects on the brain [9]. This allows researchers to compare effect sizes obtained with different imaging protocols and scanners, but also across different diseases. The notion of who qualifies as a healthy control may also depend on the dataset and may not represent the healthy population at large. If multiple datasets are used to model normal variation, then arguably diagnostic classification may be improved without retraining new models for every disease and every new dataset.

When pooling scans from patients with a variety of diseases, or at different stages of disease progression, machine learning techniques can classify the data into diagnostic groups. This may involve feature extraction, dimension reduction, model

training and testing. For example, Principal Component Analysis (PCA) uses an orthogonal linear transformation to convert observations of potentially correlated variables into a new set of linearly uncorrelated principal components (PC). New datasets can then be classified into groups based on PC-projected features. Linear discriminant analysis (LDA) can also be used for dimensionality reduction and classification. It finds a linear combination of features that optimally separates two or more classes. LDA and PCA both use linear combinations of variables to model the data. LDA models the differences between classes within the data, but PCA seeks components that have the highest variance possible under the constraint that they are orthogonal to (i.e., uncorrelated with) the preceding components [10]. These dimensionality reduction methods assume that the data form a vector space. Here, each subjects data is modeled as a vector and the collection of subjects is modeled as a single data matrix. Each column of the data matrix corresponds to one subject and each row corresponds to a feature. There are disadvantages of this vector model, as it overlooks spatial relations within the data. To overcome this, Generalized Low Rank Approximations of Matrices (GLRAM) has been proposed to use a lower dimension 2D matrix to obtain more compact representations of original data with limited loss of information [11].

In this study, we combined two different datasets collected with both standard T1-weighted MRI and DW-MRI and created connectivity networks for all study participants. Both datasets had scanned healthy controls; one had also scanned patients with Alzheimers disease and patients with early and advanced signs of mild cognitive impairment (early MCI and late MCI respectively). We merged this data hypothesizing that we could automatically classify the scans into four groups (HC, EMCI, LMCI, and AD) using brain networks as the raw features. We used GLRAM to first reduce the dimensionality, and then applied LDA in the PCA subspace to classify the data. Classification of data from multiple sites and scanners will help us to understand differences in disease progression, ideally unconfounded by scanner differences.

2 Subjects and Methods

2.1 Data Description

Table 1 summarizes the two datasets used in this study. For all datasets, participants were scanned with both DW-MRI and standard T1-weighted structural MRI.

The first dataset included 221 healthy young adults. Images were acquired with a 4T Bruker Medspec MRI scanner, using single-shot echo planar imaging with the following parameters: TR/TE = 6090/91.7ms, 23cm FOV, and a 128x128 acquisition matrix. Each 3D volume consisted of 55 2-mm axial slices, with no gap, and 1.79x1.79mm² in-plane resolution. 105 image volumes were acquired per subject:

11 with T2-weighted b0 volumes and 94 diffusion-weighted volumes ($b = 1159$ s/mm²).

The second dataset was from ADNI2, the second stage of the Alzheimers Disease Neuroimaging Initiative (ADNI), publically available online (<http://adni.loni.usc.edu>). This dataset has 199 subjects, which includes 47 healthy elderly controls, 111 with mild cognitive impairment (MCI) and 41 with Alzheimers disease (AD). Images were acquired with 3T GE Medical Systems scanners at 14 sites across North America. Each 3D volume consisted of 2.7mm isotropic voxels with a 128x128 acquisition matrix. 46 image volumes were acquired per subject: 5 T2-weighted b0 images and 41 diffusion-weighted volumes ($b = 1000$ s/mm²).

Table 1: Summary of data used in this study

	Dataset 1			Dataset 2		
Type	Number	Age	Sex	Number	Age	Sex
HC	221	24.1±2.1	85M	47	72.6±6.2	21M
EMCI	N/A			73	72.3±7.9	44M
LMCI				38	72.6±5.6	24M
AD				41	75.5±9.0	25M

2.2 Proposed framework

First, we first used GLRAM to create dimensionality-reduced matrices for each sub-ject. These new matrices were used as input to LDA on PCA for model training. Adaptive 1-nearest neighbor classification (A-1NNC) was used to label the test cases. The frameworks flowchart is shown in **Fig. 1**.

2.2.1 Brain Network Computation

In this study, we used the subjects structural networks as features for classification. To compute the brain networks, FreeSurfer (<http://freesurfer.net/>) was run on the T1-weighted images to automatically segment the cortex into 68 unique regions (34 per hemisphere). This segmentation was dilated with an isotropic box kernel of 5mm to ensure cortical labels would intersect with the white matter tissue in areas of reliable tractography for the connectivity analysis. We registered the T1-weighted intensity image to the fractional anisotropy (FA) image from the DWI data. The resultant transformations were used to transform the dilated cortical segmentations into the DWI space.

DWI images were corrected for eddy current distortions using FSL [12]. Then we used an optimized global probabilistic tractography method [13] to generate whole brain tractography for each subject. We combined the cortical segmentation and

tractography to compute a connectivity matrix for each subject. The matrices were 68×68 in dimension, corresponding to the 68 segmented cortical regions. Each cell value of the matrix represented the number of fibers that intersected pairs of cortical regions. We normalized the matrix by the total number of fibers per subject. This symmetric 68×68 matrix served as the input for our classification.

2.2.2 Data Normalization

Some form for data normalization is critical especially when working with data from different cohorts or projects, covering a wide age range. So directly pooling two datasets may introduce bias, if the proportion of controls depends on the scanner used or scanning site. To account for these confounds, we used generalized linear regression to adjust each value in the brain connectivity matrix for age, sex and scanning site. Then we further normalized the residual after regression to yield centered, scaled data, which served as the input for next step. This normalization used a Z-transformation based on the standardized statistic $Z=(X-\text{mean}(X))/\text{std}(X)$, where X is one feature vector within each dataset. For our connectivity matrix, X is $\text{element}(i,j)$ for all subjects in each dataset.

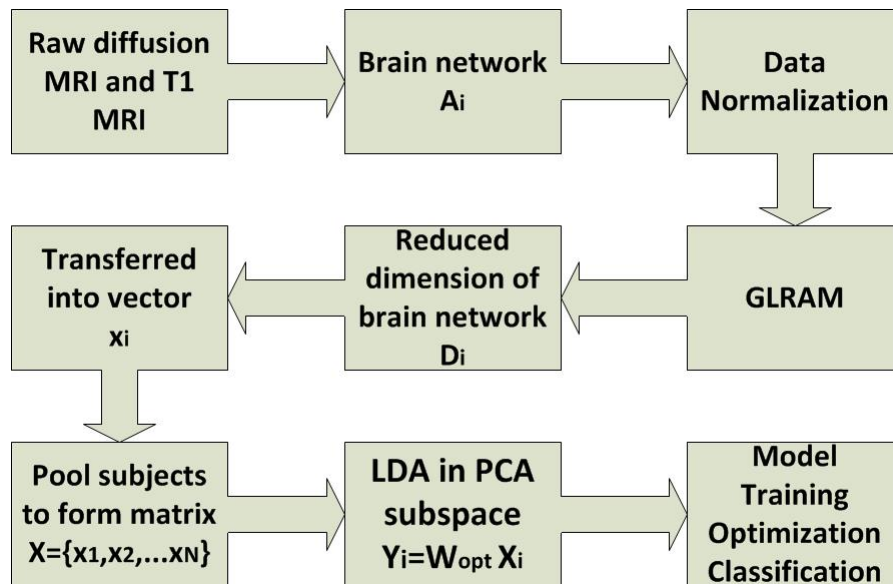


Fig. 1: Flowchart of proposed framework for connectivity based disease classification.

2.2.3 GLRAM

The purpose of GLRAM, proposed in [11], is similar to singular value decomposition (SVD) but has lower computational cost; it finds a lower rank 2D matrix D_i to approximate the original 2D matrix A_i , realizing the following function:

$$\min_{L,R,D} \sum_{i=1}^N \|A_i - LD_iR^T\|_F^2 \quad (1)$$

Here, A_i is each subjects raw brain network, N is the total number of subjects, D_i is the reduced representation of A_i ; and L and R are transformation matrices on the left and right side, respectively. F is the Frobenius norm. Details of how to solve this cost function optimization problem are in [11].

2.2.4 LDA on the PCA subspace

PCA finds linear projections that maximize the scatter of all projected samples. Mathematically, given a set of N subjects $X = \{x_1, x_2, \dots, x_N\}$, where each subject belongs to one of C classes X_1, X_2, \dots, X_C , we plan to map x_i to y_i where $y_i \in R^m$ and $m < n$. To do this, we define a linear transformation W to satisfy $y_i = W^T x_i$ ($i=1,2,N$). In PCA, the optimal projection $W_{opt-pca}$ is defined as:

$$\begin{cases} W_{opt-pca} = \arg \max_w |W^T S_T W| \\ S_T = \sum_{i=1}^N (x_i - \mu)(x_i - \mu)^T \end{cases} \quad (2)$$

Here $\mu \in R^n$ is the mean value of all samples. And $W_{opt-pca} = \{w_i \in R^n | i = 1..m\}$ is the set of eigenvectors of ST corresponding to the m largest eigenvalues. Once eigenvectors are determined, all data can be projected into this eigenspace for classification. However, PCA is not optimal for classification as the dimensions that model the greatest amount of variance in the data are not typically the ones that best differentiate groups. In other words, the discriminant dimensions could be thrown out or intermixed during PCA.

LDA seeks a projection to maximize the ratio of the determinant of the between-class scatter matrix (S_B) of the projected data to the determinant of the within-class scatter matrix (S_W) of the projected data. However, the within-class scatter matrix S_W in LDA is typically singular. This is because the number of subjects is often much smaller than the number of variables in the data. To overcome the complication of a singular S_W , we adopted the solution in [14]. In short, C is the number of classes, so we first adopted PCA to reduce the dimension of the feature space to $N-C$, and then we applied the standard LDA to reduce the dimension to $C-1$, so the transformation W_{opt} is given by:

$$\begin{cases} W_{opt} = W_{opt-pca}W_{opt-pca-lda} \\ W_{opt-pca-lda} = \arg \max_w \frac{|W^T W_{opt-pca}^T S_B W_{opt-pca} W|}{|W^T W_{opt-pca}^T S_W W_{opt-pca} W|} \\ S_B = \sum_{i=1}^C N_i (\mu_i - \mu)(\mu_i - \mu)^T \\ S_W = \sum_{i=1}^C \sum_{x_k \in X_i} (x_k - \mu_i)(x_k - \mu_i)^T \end{cases} \quad (3)$$

Where μ_i is the mean vector of class X_i , and N_i is the number of samples in class X_i . Also, $W_{opt-pca}$ can be computed using Eq. 2.

2.2.5 Adaptive 1-NNC

We classified the subjects class membership based on the Euclidean distance using 1-nearest neighbor classification (1-NNC). 1-NNC is designed to assign an object to the same class as its single nearest neighbor. Adaptive 1-NNC (A-1NNC) is a variation of 1-NNC. The test objects class membership is still decided based on the class membership of the single nearest-neighbor used for training, but once a new test objects class membership has been determined, it is grouped into training group to enhance the membership class affinity.

2.3 Experimental Procedure

The detailed procedure is described as follows:

1. Construct the brain network for each subject in both datasets.
2. Data Normalization to get input matrix A .
3. Group subjects into four classes: HC, EMCI, LMCI and AD.
4. Divide each class into three parts by randomization: training (80%), optimizing (10%) and testing (10%).
5. Pick up training dataset A_{train}
6. Set the initial dimension size to run GLRAM on A_{train} to get L_{train} , R_{train} and $D_{train} = D_1, D_2, \dots, D_N$ for each class (using **Eq. 1**)
7. Transfer D_{train} into vector x_i and form matrix $X_{train} = \{x_1, x_2, \dots, x_N\}$
8. Run LDA in PCA subspace to get W_{opt} (using Eq. 3) and get the projected data $Y_{train} = y_1, y_2, \dots, y_N = W_{opt} X$
9. Then the projection of the optimizing dataset $A_{optimizing}$ can be generated using **Eq. 4**.
10. Use A-1NNC classification to assign $Y_{optimizing}$'s class based on Y_{train} and compute the accuracy by comparing the assigned membership to ground truth
11. Then adjust the parameter in **Step 6**, re-run steps 6-10 to find the optimal parameter for the dimension of L and R in **Eq. 1** that achieves best accuracy

12. Use this optimal parameter achieved in **Step 11**, and use the test dataset to test our framework and get final grade
13. Repeat **steps 4-12** (100 times) and compute the area under the curve (AUC) for overall classification accuracy, as well as for the accuracy of each class. The higher the AUC, the better the model performance.

$$\begin{cases} D_{\text{optimizing}} = L_{\text{train}}^T A_{\text{optimizing}} R_{\text{train}} \\ D_{\text{optimizing}} \rightarrow X_{\text{optimizing}} \\ Y_{\text{optimizing}} = W_{\text{opt}} X_{\text{optimizing}} \end{cases} \quad (4)$$

3 Results and Discussion

Before we ran classification experiments, we first studied the effects of pooling datasets 1 and 2 together. A testable null hypothesis is that the feature set in the dataset 1 and dataset 2 are independent random samples drawn from Normal distributions with equal means and equal but unknown variances. As each subjects brain network is symmetric and has dimension 68×68 , we have $68 \times 67 / 2 = 2278$ features per subject. Thus we adopted False Discovery Rate (FDR) to account for the multiple comparisons (FDR $q=0.05$). Figure 2 shows the FDR-corrected P map from a Students t-test between dataset 1 (all HC) and HC from dataset 2. Our results showed that by using our proposed normalization methods, there are no detectable differences between the HCs in dataset 1 and dataset 2. Given this information, we pooled data bettering an effort to boost statistical power.

Then we compared our proposed method with the other 3 methods including: direct PCA, LDA in the PCA subspace, and GLRAM only. Table 2 shows the AUC comparison for the 4-class (HC, EMCI, LMCI and AD) classification results using dataset 2 only and then also using both datasets for defining the PCs. The results indicated that our proposed framework performed better than other methods. As shown in Table 2, PCA showed the poorest performance, which is reasonable as PCA emphasizes the data variance, which is not necessarily useful for classification. Also, GLRAM performed better than LDA. The possible explanation could be that our features were the full brain networks, which emphasized the connections between the nodes. So there may be some 2D spatial information in the features that are ignored in the vector space model (LDA). Moreover, HC classification accuracy improved when adding dataset 1, suggesting the advantage of pooling data, so long as appropriate normalization is applied.

4 Conclusion

Here we presented a novel framework using GLRAM and modified LDA to reduce the dimension of a 68×68 element structural brain connectivity network. We then

Table 2: Comparison of AUCs. A higher value indicates greater accuracy

Dataset2 Only	Overall	HC	EMCI	LMCI	AD
Direct PCA	26.19	26.50	46.47	17.50	22.44
LDA in the PCA subspace	26.31	59	21.20	9.25	13.67
GLRAM only	26.74	53.1	14.38	12.38	21.22
Proposed method	40.48	40	53.33	37.50	22.22
Dataset1+Dataset2	Overall	HC	EMCI	LMCI	AD
Direct PCA	65.43	82.36	5.25	5.75	14
LDA in the PCA subspace	66.48	90.14	5.2	2	5.11
GLRAM only	80.69	99.96	43.40	15	21.33
Proposed method	83.62	100	46.67	37.50	33.33

used Adaptive-INNC to classify patients with different stages of Alzheimers disease

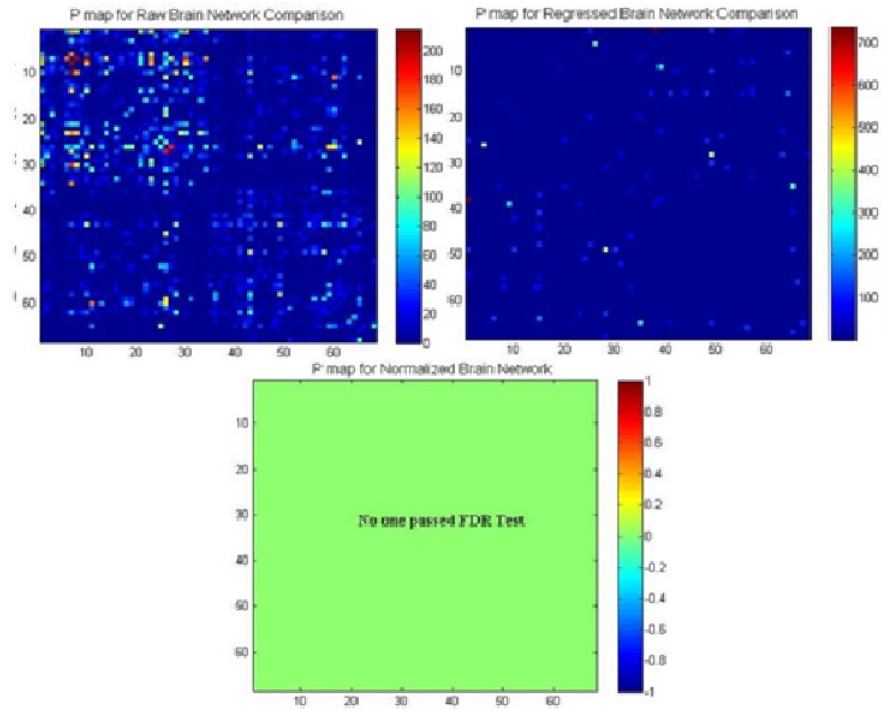


Fig. 2: An FDR-corrected P map (on a log scale) for the null hypothesis asserting that features in datasets 1 and 2 are independent random samples drawn from Normal distributions with equal means and equal but unknown variances. All P values larger than the critical FDR threshold have been set to zero. The top left map is for the raw brain networks (generated in **Section 2.2.1**). The top right map is for residual brain networks after the effects of age and sex are removed (regression on age, sex and data label, described in **section 2.2.2**). The bottom map is for normalized brain networks generated as in **Section 2.2.2**.

versus healthy controls. Our proposed method outperformed classical classification methods, but incorporating healthy controls from additional datasets also improved classification.

As our proposed framework is based on some elementary approaches (such as PCA and LDA), we compared these methods to ours, instead of other more complex approaches. In future work, we will try more sophisticated approaches. As an innovation, most current studies focus on one type disease vs. HC, while our target is for a more complicated (realistic) situation and we know there are ways to improve the proposed framework. Our current results indicate that our approach is promising.

References

1. Jessen F, Wolfsgruber S, Wiese B et al (2014) AD dementia risk in late MCI, in early MCI, and in subjective memory impairment. *Alzheimers Dement.* 10:76–83.
2. Mitchell, AJ (2009) CSF phosphorylated tau in the diagnosis and prognosis of mild cognitive impairment and Alzheimer’s disease: a meta-analysis of 51 studies. *J Neurol Neurosurg Psychiatry* 80:966–975.
3. Aisen PS, Petersen RC, Donohue MC et al (2010) Clinical Core of the Alzheimer’s Disease Neuroimaging Initiative: progress and plans. *Alzheimers Dement* 6:239–246.
4. Winblad B, Palmer K, Kivipelto M et al (2004) Mild cognitive impairment—beyond controversies, towards a consensus: report of the International Working Group on Mild Cognitive Impairment. *J Intern Med* 256:240–246.
5. LeBihan, D (1990) IVIM method measures diffusion and perfusion. *Diagn Imaging (San Franc)* 12:133–136.
6. Sporns, O (2011) The human connectome: a complex network. *Ann N Y Acad Sci* 1224:109–125.
7. Ajilore, O, Lamar M, Leow A et al (2014) Graph Theory Analysis of Cortical-Subcortical Networks in Late-Life Depression. *Am J Geriatr Psychiatry.* 22:195–206.
8. Zhang, J., Cheng W., Wang Z et al (2012) Pattern classification of large-scale functional brain networks: identification of informative neuroimaging markers for epilepsy. *PLoS One* 7:e36733.
9. Thompson, PM., Stein JL, Medland SE et al (2014) The ENIGMA Consortium: large-scale collaborative analyses of neuroimaging and genetic data. *Brain Imaging Behav* 8:153–162.
10. Wang, J., Zhou L (2011) Research on magnetoencephalography-brain computer interface based on the PCA and LDA data reduction. *Sheng Wu Yi Xue Gong Cheng Xue Za Zhi* 28:1069–1074.
11. Ye, J. (2005) Generalized Low Rank Approximations of Matrices. *Mach. Learn.* 61:167–191.
12. Jenkinson M, Beckmann CF, Behrens TE et al. (2012) FSL. *Neuroimage* 62:782–790
13. Aganj, I, Lenglet C, Jahanshad N et al (2011) A Hough transform global probabilistic approach to multiple-subject diffusion MRI tractography. *Med Image Anal* 15:414–425
14. Belhumeur PN, Hespanha JP, Kriegman DJ (1997) Eigenfaces vs. fisherfaces: Recognition using class specific linear projection. *Pattern Analysis and Machine Intelligence, IEEE Transactions on* 19:711–720.

Contents

Part I Network Analysis

Vector Weights and Dual Graphs: An Emphasis on Connections in Brain Network Analysis	3
Peter Savadjiev, Carl-Fredrik Westin, and Yogesh Rathi	

Rich Club Network Analysis Shows Distinct Patterns of Disruption in Frontotemporal Dementia and Alzheimer’s Disease	13
Madeline Daianu, Neda Jahanshad, Julio E. Villalon-Reina, Mario F. Mendez, George Bartzokis, Elvira E. Jimenez, Aditi Joshi, Joseph Barsuglia, and Paul M. Thompson	

Parcellation-Independent Multi-Scale Framework for Brain Network Analysis	23
M.D. Schirmer, G. Ball, S.J. Counsell, A.D. Edwards, D. Rueckert, J.V. Hajnal, and P. Aljabar	

Part II Clinical Applications

Multiple Stages Classification of Alzheimer’s Disease Based on Structural Brain Networks Using Generalized Low Rank Approximations (GLRAM)	35
L. Zhan, Z. Nie, J. Ye, Y. Wang, Y. Jin, N. Jahanshad, G. Prasad, G.I. de Zubicaray, K.L. McMahon, N.G. Martin, M.J. Wright, and P.M. Thompson	

The Added Value of Diffusion Tensor Imaging for Automated White Matter Hyperintensity Segmentation	45
Hugo J. Kuijf, Chantal M.W. Tax, L. Karlijn Zaanen, Willem H. Bouvy, Jeroen de Bresser, Alexander Leemans, Max A. Viergever, Geert Jan Biessels, and Koen L. Vincken	

Algebraic Connectivity of Brain Networks Shows Patterns of Segregation Leading to Reduced Network Robustness in Alzheimer’s Disease	55
Madelaine Daianu, Neda Jahanshad, Talia M. Nir, Cassandra D. Leonardo, Clifford R. Jack Jr., Michael W. Weiner, Matt A. Bernstein, and Paul M. Thompson	
Diffusion-Map: A Novel Visualizing Biomarker for Diffusion Tensor Imaging of Human Brain White Matter	65
Mohammad Hadi Aarabi and Hamid Saligheh Rad	
A Multi-Parametric Diffusion Magnetic Resonance Imaging Texture Feature Model for Prostate Cancer Analysis	79
Farzad Khalvati, Amen Modhafar, Andrew Cameron, Alexander Wong, and Masoom A. Haider	
Predicting Poststroke Depression from Brain Connectivity	89
J. Mitra, K.-K. Shen, S. Ghose, P. Bourgeat, J. Fripp, O. Salvado, B. Campbell, S. Palmer, L. Carey, and S. Rose	
Part III Tractography	
Fiber Bundle Segmentation Using Spectral Embedding and Supervised Learning	103
Dorothee Vercruysse, Daan Christiaens, Frederik Maes, Stefan Sunaert, and Paul Suetens	
Atlas-Guided Global Tractography: Imposing a Prior on the Local Track Orientation	115
Daan Christiaens, Marco Reisert, Thijs Dhollander, Frederik Maes, Stefan Sunaert, and Paul Suetens	
Part IV Q-space Reconstruction	
Magnitude and Complex Based Diffusion Signal Reconstruction	127
Marco Pizzolato, A. Ghosh, Timothé Boutelier, Rachid Deriche	
Diffusion Propagator Estimation Using Gaussians Scattered in q-Space	141
Lipeng Ning, Oleg Michailovich, Carl-Fredrik Westin, and Yogesh Rathi	

An Analytical 3D Laplacian Regularized SHORE Basis and Its Impact on EAP Reconstruction and Microstructure Recovery 151
 Rutger Fick, Demian Wassermann, Gonzalo Sanguinetti, and Rachid Deriche

Part V Post-processing

Motion Is Inevitable: The Impact of Motion Correction Schemes on HARDI Reconstructions 169
 Shireen Elhabian, Yaniv Gur, Clement Vachet, Joseph Piven, Martin Styner, Ilana Leppert, G. Bruce Pike, and Guido Gerig

Joint Super-Resolution Using Only One Anisotropic Low-Resolution Image per q-Space Coordinate 181
 Vladimir Golkov, Jonathan I. Sperl, Marion I. Menzel, Tim Sprenger, Ek Tsoon Tan, Luca Marinelli, Christopher J. Hardy, Axel Haase, and Daniel Cremers

Bilateral Filtering of Multiple Fiber Orientations in Diffusion MRI 193
 Ryan P. Cabeen and David H. Laidlaw

Dictionary Based Super-Resolution for Diffusion MRI 203
 Burak Yoldemir, Mohammad Bajammal, and Rafeef Abugharbieh

Index 215



<http://www.springer.com/978-3-319-11181-0>

Computational Diffusion MRI

MICCAI Workshop, Boston, MA, USA, September 2014

O'Donnell, L.; Nedjati-Gilani, G.; Rathi, Y.; Reisert, M.;

Schneider, T. (Eds.)

2014, IX, 219 p. 63 illus., 51 illus. in color., Hardcover

ISBN: 978-3-319-11181-0